



## *Neutronic performance of accident tolerant fuels in system-integrated modular advanced reactor (SMART)*

Karimi Jafari A.<sup>1</sup>, Khoshahval F.<sup>2,\*</sup>

<sup>1</sup>Science and Research Branch, Islamic Azad University, P.O.Box: 14778-93855, Tehran - Iran.

<sup>2</sup>Reactor and Nuclear Safety Research School, Nuclear Science and Technology Research Institute (NSTRI), P.O.Box: 14155-1339, Tehran – Iran

\* Email of the corresponding author: [f\\_khoshahval@sbu.ac.ir](mailto:f_khoshahval@sbu.ac.ir)

### **Abstract**

After the Fukushima Daiichi, many methods have been considered to improve the neutronic and thermo-hydraulic performance of the nuclear power plants. In this investigation, the system integrated modular advanced reactor (SMART) as a new innovative designed reactor is chosen as a case study. The commercial fuel (UO<sub>2</sub>) is changed with the U<sub>3</sub>Si<sub>2</sub>, UC, and UN to analyze the steady-state core parameters. The neutronic analysis of the reactor core is performed using the DRAGON/PARCS codes. The results predict the behavior of the core through the effective multiplication factor ( $K_{eff}$ ) versus effective full power days (EFPDs), which leads to a longer cycle length for the SMART core fueled with U<sub>3</sub>Si<sub>2</sub> and UC about 51% and 29%, respectively. In addition, the fuel temperature coefficient (FTC) and moderator temperature coefficient (MTC) form a negative feedback effect.

**Keywords:** ATF, SMR, U<sub>3</sub>Si<sub>2</sub>, UC, UN

### **1 Introduction**

The fuel for nuclear reactors has been continuously developing for nearly 50 years and is one of the main components. In the framework of fuel development, the focus was not just on economics, but also regarding safety to protect the reactor from possible accidents. Nuclear power plants (NPPs) have used uranium dioxide fuel clad with zirconium alloy (traditional fuels) for decades. Due to such nuclear accidents that include Fukushima Daiichi (2011) and Three Mile Island (1979) severe disaster, the relatively poor thermal conductivity of the traditional fuels lead to a high temperature and heat accumulation inside it, which may causes the fuel melts in a nuclear reactor. Besides, zirconium alloy reacts with coolant water at high temperatures and this reaction produces hydrogen [1, 2].

The preferred accident tolerant fuel (ATF) attributes highlight the overall performance of each fuel and cladding under regular and postulated accident conditions. Fuel system layout options need to first hold desirable cladding and fuel thermo-mechanical properties, fuel-clad interactions, and fission product behavior. Targeting upgrades in those attributes courses in organizing the critical parameters that should be taken into consideration withinside the improvement of fuels and cladding with more suitable accident tolerance. Accident tolerant attributes consist of decrease hydrogen generation rate (or generation of different flammable gases), and decreased stored

energy when compared to the traditional fuel systems. [3,4].

The layout flexibility of small modular reactors (SMRs) in synergy with ATFs affords an extended time to react to the lack of active cooling under severe accidents and gives comparable fuel overall performance throughout normal operation. Managing the safe, efficient, and reliable production of energy using SMRs may be an excellent solution for developing countries without the infrastructure to build large NPPs. Furthermore, these small reactors deliver electricity in remote areas that require smaller and localized power centers, which eliminates the need for long and expensive transmission lines. Another benefit of an SMR is that it could deliver water through the desalination process to local areas facing a water rarity [5,6].

Numerous factors of ATFs are being studied, include methods wherein the cost of this new technology can be offset. ATFs are focused on current Generation II and III light water reactors (LWRs). further, they might be of a hobby for Gen III heavy water reactors (HWRs), water-cooled SMRs, and in the future for Gen IV in particular the supercritical water reactor (SCWR). There are also predicted applications for some ATF materials for Gen IV fast reactors, ATF technology may also be utilized, across all current/future reactor types, with fuels containing plutonium (Pu) and/or minor actinides (MAs), including those which have the capacity for use in future sustainable closed fuel cycles [7].



In this study, Uranium Silicide ( $U_3Si_2$ ), Uranium Carbide (UC), Uranium Nitride (UN), and Uranium dioxide ( $UO_2$ ) were investigated as fuel materials with  $^{235}U$  enriched to 4.95 % for SMART [8].  $U_3Si_2$ , UC, and UN are potential fuels for future applications due to their higher thermal conductivity, melting points, and uranium content compared with  $UO_2$ .

## 2 Accident tolerant fuels

The ATF's are described as fuels that could tolerate a severe accident in the reactor core for an extended time. The main problem of the traditional fuel is its comparatively poor neutronic, thermal-hydraulic, and solid mechanics performance.  $UO_2$  has lower thermal conductivity lead to a high temperature and a high heat accumulation inside it, which reasons partial melt-down for fuel material. Besides, zirconium alloys will react with water at high temperatures that result in the generation of hydrogen which will cause a massive explosion at the plant. So, the demand for new fuel materials becomes imperative to overcome the traditional fuel problems.

The candidate ATF's can be divided into two categories: improved technology and innovative technology. Improved technology is based on the traditional fuel current technology with performance improvement and innovative technology uses a new uranium compound, such as  $U_3Si_2$  and UN alloy.

Table 1. The propertise of the materials[12,13]

Material	Density (g/Cm <sup>3</sup> )	Conductivity (W/mK)	Melting point (K)
$U_3Si_2$	11.59	48	1938
UC	13.63	19	2780
UN	13.59	21.5	3055
$UO_2$	10.41	~ 4	2873

Table 1 is shown the thermal conductivity, density, and melting point of  $U_3Si_2$ , UC, and UN candidates of fuel materials.

$U_3Si_2$  is one of the most promising fuels with higher thermal conductivity and heavy metal density than  $UO_2$ , which might also additionally decrease operation temperature, increase power density or even extend the core lifetime. Due to its higher thermal conductivity, the temperatures in the fuel center could be significantly much less affected by the reactor operation, and the stored heat of the fuel could be reduced. The thermal conductivity of  $U_3Si_2$  will increase with its temperature, even as that of  $UO_2$  decreases. So, the thermal conductivity of  $U_3Si_2$  is continually better than  $UO_2$  at LWR operating temperature [9].

The use of UN fuel in light water reactors has lately obtained increasing interest because of its capability

advantages. According to the Table 1, It has a higher density, thermal conductivity, and melting point than  $UO_2$ . However, it's far still difficult to attain a long sufficient cycle length. From the neutronic point of view,  $^{14}N$  has an excessive thermal neutrons absorption cross-section, to have an effect on the numerous neutronic parameters and could now produce an appropriate no longer neutronic overall performance as compared to the traditional fuel materials. A high-priced enrichment system may be carried to an increase of  $^{15}N$ , which has a low thermal neutron absorption cross-section, to conquer this problem. Its thermal conductivity is better than the thermal conductivity of  $UO_2$ . So, UN fuel material will reduce the high fuel temperature and heat accumulation troubles that cause partial fuel melt-down accidents [10].

Due to the fact for numerous reasons, UC is an attractive opportunity for  $UO_2$  as a fuel material. The first is its superiority of thermo-physical properties. Secondly, UC reveals suitable dimensional balance and fission gas retention throughout irradiation. Thirdly, it's far chemically strong with the coolant and capacity cladding materials. UC has a better density and thermal conductivity than  $UO_2$ . So, the thermal-hydraulic overall performance of the UC might be the nice one of them. For the neutronic analysis,  $^{12}C$  has a totally low thermal-neutron absorption cross-section. These properties offer operation at better power density, which reasons a reduction in reactor core size, and subsequently a reduction in capital cost [11].

## 3 Case study description

SMART is a soluble boron-free small advanced integral pressurized water reactor with the capability of producing 90-100 MWe designed by the Korea atomic energy research institute (KAERI). The integrated design adds some inherent and passive safety features to the reactor. The reactor is considered a cost-effective solution due to its modular construction that makes it even a feasible tool for water desalination in addition to electrical power generation. As an example, the reactor can provide 40000 m<sup>3</sup>/day desalinated water with only 10% of its daily energy supply [14]. SMART contains eight steam generators, a pressurizer, four reactor coolant pumps, and twenty-five control rod drive mechanisms in a single pressurized reactor vessel.

The core consists of 57 fuel assemblies, which are designed and proven by Korea fuel assemblies (KOFA) industries based on a 17×17 square arrangement. Each of the fuel assemblies consists of 264 fuel and burnable-absorber rods, 24 thimbles for the guide tube, and 1 thimble at the center for instrumentation. Fuel rods consist of 4.95% uranium enrichment and burnable-absorber rods consist of 4 w.t. % natural  $Gd_2O_3$  and 1.8% uranium enrichment.

Also,  $\text{Al}_2\text{O}_3\text{-B}_4\text{C}$  rods with different amounts of  $^{10}\text{B}$  have been used as shim rods in fuel assemblies [15]. Figure 1 shows the core loading pattern and Table 2 illustrated the number of several rods in each type of fuel assemblies.

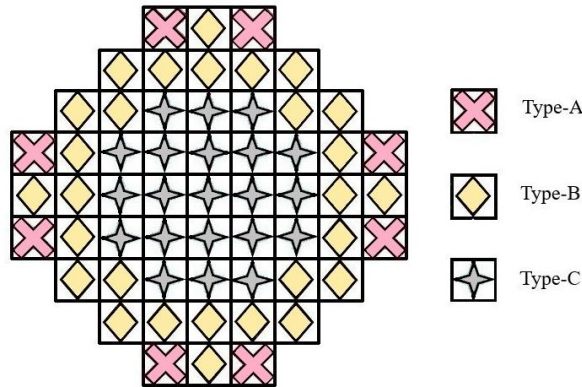


Figure 1. Core loading pattern of SMART

Table 2. Number of different cells in each fuel assembly

Cell type	Type-A	Type-B	Type-C
Instrumentation and guide tube	25	25	25
Fuel rod (4.95 % $^{235}\text{U}$ enrichment)	224	240	236
Barnable-Absorber rod (4 w.t. % $\text{Gd}_2\text{O}_3$ & 1.8 % $^{235}\text{U}$ enrichment)	12	4	4
$\text{Al}_2\text{O}_3\text{-B}_4\text{C}$ rod ( $\text{B}^{10}$ : 0.01110 g/cm)	28	0	0
$\text{Al}_2\text{O}_3\text{-B}_4\text{C}$ rod ( $\text{B}^{10}$ : 0.01588 g/cm)	0	16	8
$\text{Al}_2\text{O}_3\text{-B}_4\text{C}$ rod ( $\text{B}^{10}$ : 0.02900 g/cm)	0	0	8
$\text{Al}_2\text{O}_3$ rod	0	4	8

#### 4 Calculation methods

The method applied for neutronic calculation is divided into two main steps, including lattice calculation and core calculation. Simulation of lattice and core performed using DRAGON-v4 [16] and PARCS-v3 [17], respectively.

The computer code DRAGON is a lattice code designed around solution techniques of the neutron transport equation. The DRAGON project results from an effort made at Ecole Polytechnique de Montreal to rationalize and unify into a single code the different models and algorithms used in a lattice code. One of the main concerns was to ensure that the structure and implementation of new calculation techniques would be facilitated. DRAGON is therefore a lattice cell code that is divided into many calculation modules linked together using the GAN generalized driver. These modules exchange information only via well-defined data structures [16].

PARCS is a reactor core simulator in 3D which solves the steady-state and time-dependent, neutron diffusion and low order transport equations in orthogonal and non-orthogonal geometries. In PARCS, the input system is based on the name of the card, so that the use of more default input parameters and the amount of data entered into the system is reduced. Various editing options are available in PARCS that illustrate many different aspects of the computational results. To calculate fuel depletion and burnup, macroscopic cross-sections are needed and created by the lattice calculation code output [17].

Thus, according to the structure and arrangement of fuel rods, modeling of different fuel assemblies was done using DRAGON calculation code followed by extracting group coefficients (transport, scattering, absorption, and fission cross-sections) related to each cell. Finally, using calculated data as PMAXS file input to the PARCS core calculation Code, then, neutronic values (flux distribution, power peaking factor, and  $K_{\text{eff}}$ ) are calculated for the entire reactor core.

#### 5 Neutronic analysis results

##### 5.1 Effective multiplication factor

The  $K_{\text{eff}}$  at the beginning of the cycle (BOC) was reported by CASMO-3\MASTER and MCNAP Codes at the hot full power (HFP) condition equal to 1.05588 and 1.06178, respectively [18] and the maximum fuel cycle length for the  $\text{UO}_2$  fuel material is reported as 990 EFPDs [19].

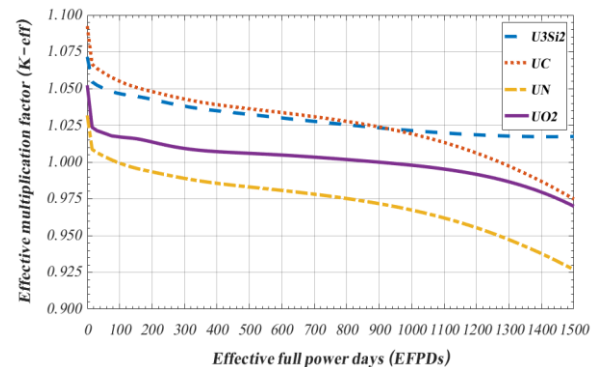


Figure 2.  $K_{\text{eff}}$  versus EFPDs for types of materials

Figure 2 shows that the core cycle length with UN, UC, and  $\text{U}_3\text{Si}_2$  fuel materials are 100, 1280, and 1500 EFPDs, respectively. Also, Table 3 represents  $K_{\text{eff}}$  at the BOC for the four fuel materials by DRAGON/PARCS calculation methods.

Table 3.  $K_{\text{eff}}$  at the BOC for each fuel material

Parameter	Fuel material			
	UN	$\text{UO}_2$	UC	$\text{U}_3\text{Si}_2$
$K_{\text{eff}}$	1.031824	1.052241	1.092509	1.071676

At the BOC, there are differences between the  $K_{eff}$  values of  $UO_2$  with UN, UC, and  $U_3Si_2$ . The reason for these differences is that the atomic density of  $^{235}U$  in the cases of these materials is greater than that in  $UO_2$ . Despite the high density of the UN fuel, the  $K_{eff}$  of the reactor core is lower than the others, which is because of the high thermal neutron absorption cross-section of the  $^{14}N$  in natural nitrogen.

### 5.2 Radial Power distribution

Figure 3 shows the radial power distribution values for the one-eighth symmetry of the core at the HFP. The first line shows the values calculated by DRAGON/PARCS codes, the second and third lines show the CASMO-3/MASTER and MCNAP reported values [20]. As shown in Figure 3, the maximum power is obtained in the central FA and the minimum power is obtained in the corner FA, which has the highest amount of gadolinium.

1.462	1.415	1.282	1.075	0.640
1.487	1.444	1.316	1.117	0.613
1.515	1.468	1.327	1.121	0.602
	1.370	1.237	0.996	0.475
	1.400	1.262	1.012	0.429
	1.422	1.270	1.007	0.418
DRAGON/PARCS	1.128	0.778		
CASMO-3/MASTER	1.139	0.721		
MCNAP	1.133	0.705		

Figure 3. Power distribution for core symmetry of one-eighth

1.462	1.415	1.282	1.075	0.640
1.435	1.391	1.268	1.077	0.660
1.409	1.370	1.256	1.074	0.671
1.408	1.369	1.257	1.076	0.670
	1.370	1.237	0.996	0.475
	1.350	1.225	1.000	0.502
	1.331	1.216	1.002	0.518
	1.332	1.218	1.003	0.514
UO2	1.128	0.778		
U3Si2	1.120	0.785		
UN	1.121	0.802		
UC	1.123	0.801		

Figure 4. Power distribution for core with the different type of fuel material

Figure 4 represents the radial power distribution at the BOC for one-eighth of the proposed cores and the concept of symmetry can be used to model power distribution for the whole core. It can be deduced that the core with  $UO_2$  as a fuel material gives the maximum power peaking factor (PPF), which is equal to 1.462. While the fuel assembly with  $U_3Si_2$  as a fuel material gives PPF equal to 1.435 at the same assembly. Also, the PPF in the core with the UN and

UC fuel materials is equal to 1.409 and 1.408, respectively.

It can be obtained from figure 4, the PPF of the fuel assemblies (FAs) in the core with the UN and UC is lower and higher than the core with  $UO_2$  and  $U_3Si_2$  for the central and side FAs, respectively. It shows that the power distribution in the core with the UN and UC is more flattened than the core with  $UO_2$  and  $U_3Si_2$ .

### 5.3 Axial thermal neutron flux

Figure 5 shows the variation of the thermal neutron flux with the axial core distance for the investigated cores.

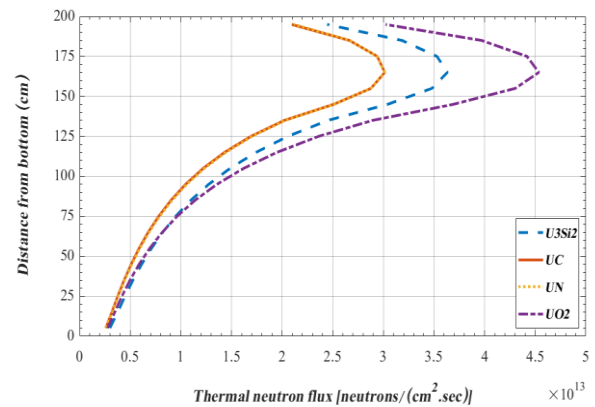


Figure 5. Axial thermal neutron flux distribution

As can be obtained from Figure 5, the higher axial thermal flux occurred in the core loaded with  $UO_2$  because of its lower density. In contrast, the lower core axial flux happened in the core with UN and UC, which have higher density compared to  $UO_2$ . Likewise,  $U_3Si_2$  density is between the density of  $UO_2$  and UN, which causes the axial flux of  $U_3Si_2$  within the range between UN and  $UO_2$ .

It is observed that the thermal flux distributions are maximum at the top of the core ( $Z=162$ ) for all fuel materials and they decrease with sinusoidal cosine shape, which is because of a more amount of  $^{10}B$  isotope at the bottom of the core [18].

### 5.4 Reactivity coefficients

Reactivity coefficients indicate the magnitude of feedback effects to core reactivity when the reactor parameters change, including fuel temperature, moderator temperature, coolant density, and etc. In reactor design, all the reactivity coefficients must be kept negative. The two most important reactivity coefficients including FTC and MTC are calculated for these types of fuel materials.

FTC is defined as the change of reactivity since the 1 K change in fuel temperature, also named doppler temperature coefficient. In most cases, because of the doppler broadening of the neutron cross-section for the fuel material as its temperature rises, the resonance



absorption increases, and thus  $K_{\text{eff}}$  falls making a negative FTC.

MTC is defined as the change of reactivity since the 1 K change in moderator temperature. In PWR, light water is implemented as both the moderator and the coolant. With the moderator temperature rising, the density of the moderator decreases which will reduce the parasitic absorption. On the other hand, the moderate capacity will be weaker and thus enhance the resonance absorption. Hence, the negativity of the MTC increases when the moderator temperature increase.

**Table 4.** FTC and MTC safety parameters values at BOC

Reactivity coefficient	Fuel material			
	UN	UO <sub>2</sub>	UC	U <sub>3</sub> Si <sub>2</sub>
FTC	-2.4242	-2.3048	-2.2642	-2.0953
MTC	-54.1361	-52.0857	-45.9551	-52.2293

The FTC depends mainly on the amount of fertile material used in the fuel. When the fuel temperature increases, more neutrons are absorbed by <sup>238</sup>U. Therefore, the higher density of the UN causes the highest FTC negativity value of the SMART core fueled with this material.

At the same increase in the moderator temperature, the MTC value changes from one fuel to another according to the type of fuel material and the concentration of the fissile material. The negativity of the MTC in the case of the UN is higher than the other investigated fuel types because of its high atomic density of the fissile atoms (<sup>235</sup>U) and the highest thermal neutron absorption cross-section of <sup>14</sup>N compared with others.

## 6 Conclusions

From the neutronic point of view, the fuel cycle length for U<sub>3</sub>Si<sub>2</sub>, UC, UO<sub>2</sub>, and UN was 1500, 1280, 990, and 100 effective full power days (EFPDs), respectively. So, U<sub>3</sub>Si<sub>2</sub> and UC as fuel materials are more economical.

FTC and MTC values of these fuel materials are negative at the BOC. The UN has highest MTC and FTC values. However, using UN fuel causes the lowest cycle length.

The U<sub>3</sub>Si<sub>2</sub> has acceptable FTC and MTC negative values, a higher cycle length, and axial thermal neutron flux lower than UO<sub>2</sub>. Despite the melting point of U<sub>3</sub>Si<sub>2</sub> fuel being smaller than others but having a higher thermal conductivity that will not cause the fuel center temperature to rise and melt. So, it can be observed as new fuel material for SMART in future research.

## References

- [1] Costa, Diogo Ribeiro, et al. "UN Microspheres Embedded in UO<sub>2</sub> Matrix: An Innovative Accident Tolerant Fuel." *Journal of Nuclear Materials*, vol. 540, 2020.
- [2] Pourrostan, A., et al. "Core Analysis of Accident Tolerant Fuel Cladding for SMART Reactor under Normal Operation and Rod Ejection Accident Using DRAGON and PARCS." *Nuclear Engineering and Technology*, vol. 53, no. 3, Elsevier Ltd, 2021, pp. 741–51.
- [3] Ebrahimgol, H., et al. "Evaluation of Accident Tolerant Cladding Materials in a Severe Accident of the BNPP." *Annals of Nuclear Energy*, vol. 129, Elsevier Ltd, 2019, pp. 214–23.
- [4] Zhou, Wei, and Wenzhong Zhou. "Enhanced Thermal Conductivity Accident Tolerant Fuels for Improved Reactor Safety – A Comprehensive Review." *Annals of Nuclear Energy*, vol. 119, Elsevier Ltd, 2018, pp. 66–86.
- [5] Locatelli, Giorgio, et al. "Small Modular Reactors: A Comprehensive Overview of Their Economics and Strategic Aspects." *Progress in Nuclear Energy*, vol. 73, 2014, pp. 75–85.
- [6] Hidayatullah, H., et al. "Design and Technology Development for Small Modular Reactors - Safety Expectations, Prospects and Impediments of Their Deployment." *Progress in Nuclear Energy*, vol. 79, no. 2015, 2015, pp. 127–35.
- [7] Oak Ridge. "Accident Tolerant Fuel Concepts for Light Water Reactors." *IAEA Tecdoc Series*, vol. 1797, no. October 2014, pp. 13–16.
- [8] IAEA. *System-Integrated Modular Advanced Reactor (SMART)*. 2011, pp. 1–36.
- [9] Liu, Rong, et al. "Multiphysics Modeling of Accident Tolerant Fuel-Cladding U<sub>3</sub>Si<sub>2</sub>-FeCrAl Performance in a Light Water Reactor." *Nuclear Engineering and Design*, vol. 330, no. February, Elsevier, 2018, pp. 106–16.
- [10] Al-Qasir, Iyad, et al. "Thermal Neutron Scattering Kernels for Uranium Mono-Nitride: A Potential Advanced Tolerant Fuel Candidate for Light Water Reactors." *Annals of Nuclear Energy*, vol. 127, Elsevier Ltd, 2019, pp. 68–78.
- [11] Pandya, Jalaja, et al. "Dependence of Strain on the Thermoelectric Properties of Uranium Carbide." *Materials Today: Proceedings*, vol. 47, Elsevier Ltd, 2020, pp. 571–75.
- [12] Pino-Medina, Sadiel, and Juan Luis François. "Neutronic Analysis of the NuScale Core Using Accident Tolerant Fuels with Different Coating Materials." *Nuclear Engineering and Design*, vol. 377, no. February, Elsevier B.V., 2021, p. 111169.
- [13] Mohsen, Mohamed Y. M., et al. "Integrated Analysis of VVER-1000 Fuel Assembly Fueled with Accident Tolerant Fuel (ATF) Materials." *Annals of Nuclear Energy*, vol. 159, Elsevier Ltd, 2021, p. 108330.
- [14] Park, Sang Yoon, et al. *Nuclear Design Report for System-Integrated Modular Advanced Reactor*. 2002.
- [15] Zee, Sung Quun, et al. 'Development of Design Technology for Integral Reactor', (2002), 563 (In Korean).
- [16] Marleau, G, et al. 'A User Guide for DRAGON', 2012, 1–276.
- [17] Downar, T. J., et al. 'PARCS v3.0 U.S. NRC Core Neutronics Simulator USER MANUAL', 2 (2010), 1–161.
- [18] Chang, M. H., et al. *Basic Design Report of SMART*. 2002 (In Korean).
- [19] Lee, Chungchan, et al. 'Nuclear and Thermal-Hydraulic Design Characteristics of the SMART Core', GENES4/ANP2003, Seminar, 2003, 15–19.
- [20] Kim, Chang Hyo, et al. *Development of core design/analysis technology for integral reactor; Verification of SMART Nuclear Design by Monte Carlo Method*, KAERI, 2002 (In Korean).